Chapter 4

The Earth's response to loading and the effect on sea-level

Any redistribution of mass on the Earth's surface on length scales of the thickness of the lithosphere (∼100 km) or greater potentially results in a deformation of the crust, a change in its gravity field, a variation in sea level, as well as a modification of the Earth's rotation. This thesis focuses on the change in mass of mountain glaciers and the effect this has on geodetic signals. However, a number of other processes, such as tectonic activity, erosion, and even man-made signals such as water retention in dams can contribute to these observational signals to varying degree. To formulate the response of the Earth to the redistribution of mass, a number of variables need to be constrained. These include the rheology of the Earth and the changes in surface loads in time and space. Geological and geomorphological evidence of past sea-level changes have been used in a range of models to constrain past ice-sheet histories and global and regional models describing the rheology of the Earth (Nakada and Lambeck, 1987; Lambeck and Nakada, 1990; Mitrovica and Peltier, 1991; Johnston, 1993b; Lambeck, 1993; Milne et al., 1999; Lambeck et al., 2000; Milne et al., 2002; Peltier, 2002; Mitrovica and Milne, 2003; Lambeck et al., 2003; Stocchi et al., 2005). In this thesis, geodetic signals are calculated from the Earth's response as a result of recent mountain deglaciation and associated sea-level changes are presented.

Section 4.1 discusses a mathematical solution that is commonly used to approximate the Earth's rheology and which will be used in this thesis. Section 4.2 describes the Earth's response to surface loading and the physical characteristics of Earth models used throughout this study. Section 4.3 discusses the contributing

factors that determine the spatial and temporal variability of sea-level changes and illustrates these changes as a result of recent mountain deglaciation using a case scenario from Svalbard, Norway.

4.1 Earth rheology

Per definition, stress is a measure of the average amount of force exerted per unit area. This applied force results in a deformation, i.e. a change in the shape and size, of the object and this deformation is often described in terms of strain. The Earth is constantly deforming and moving under a changing stress field. Of these movements, most obvious to us are probably the ocean and Earth tides (Melchior, 1983). Hence, it is clear that the Earth does not behave entirely as a rigid body (defined as a body in which the distance between any two points remains constant in time).

For the present purpose it is believed that the most convenient description of the Earth is as a viscoelastic body (e.g. Nakada and Lambeck, 1987). The two basic components of this description are *elastic* and *viscous* behaviour, commonly represented as the spring and dashpot, respectively. Elastic behaviour means that the material deforms instantaneously under stress and returns to its original size and shape when the stress is released. Hence, there is no permanent deformation. Elastic behaviour is described with Hooke's law, which relates the stress σ to strain ε proportionally. The modulus of elasticity E is a constant of proportionality and is defined by

$$\sigma_{ij} \;=\; E_{ijkl}\,\varepsilon_{kl} \tag{4.1}$$

with units of Pascal (or Newtons per square meter). The variables σ and ε are three-dimensional tensors and E is a 4^{th} order tensor containing 81 elastic coefficients (of which only 21 are independent). Dependent on how stress and strain are measured and the direction, there are different types of elastic moduli, of which five are commonly used. These are the Young's- and bulk modulus, Poisson's ratio, and the two Lamé's constants (the Lamé's constant μ, also called shear- or rigidity modulus, is defined as the ratio of shear stress to shear strain in elastic deformation; rigidity is an elastic property of a material which measures the resistance to an applied stress tending to distort the shape). The elastic properties of isotropic materials can be completely described by any two of these moduli. All other elastic moduli can be calculated as a combination of the known pair. Lateral variations in elastic moduli

may be present but have so far been difficult to measure because of limitations of the data. Rocks (as well as metals and ceramics) behave elastically at "low enough" temperatures, small strains, and rapid loading.

Materials behave viscously when they deform steadily under stress. Viscous strains are irreversible, i.e. they remain when the stress is removed. By definition, viscous behaviour relates the stress σ proportionally to the strain rate $\dot{\varepsilon}$. The constant of proportionality is the viscosity η of the material

$$\sigma_{ij} \;=\; \eta_{ijkl}\,\dot{\varepsilon}_{kl} \tag{4.2}$$

with the unit Pascal-seconds [Pa-s]. This is a measure of the resistance of a fluid to deformation under shear stresses. Purely viscous materials, like liquids, deform under the smallest stress. In contrast, while rocks do not flow under low stress, they exhibit viscous flow behaviour under high temperature and pressure. Geological observations have demonstrated that isostatic rebound, in areas such as Scandinavia and the Hudson Bay region, continued long after the deglaciation ceased. This delayed response to the removal of surface loads is the fingerprint of the viscous component in the Earth's response. Hence, viscosity is one of the important properties of the Earth, controlling not only the rate of glacial rebound, but also tectonics and other dynamic processes such as mantle convection.

Combining the elastic and viscous behaviour leads to a constitutive law for viscoelastic materials. The model used in isostatic rebound studies is the so-called *Maxwell* model

$$\dot{\varepsilon} \;=\; \frac{\dot{\sigma}}{E} \;+\; \frac{\sigma}{\eta} \tag{4.3}$$

For a detailed description of the constitutive equation of viscoelastic materials see the studies of Cathles (1975), Flügge (1975), Johnston (1993a), and Purcell (1997).

Depending on the change of strain rate versus stress inside a material, the viscosity can be categorized as having a linear, non-linear, or plastic response. When a material exhibits a linear response it is categorized as a *Newtonian* material. In this case the deformation rate is directly proportional to the stress applied. Many materials however exhibit a non-linear response to the stress and are called non-Newtonian materials. In addition, when the stress is independent of this strain rate, the material exhibits plastic deformation.

4.2 Viscoelastic Earth under surface loads

The uppermost layer of the Earth is sufficiently cold and rigid that it acts as an elastic layer when responding to surface loads, even when the loading occurs over long (millennia) times scales. This layer is commonly referred to as the lithosphere and includes the crust and the uppermost part of the mantle. The underlying mantle, which is warmer and more ductile, also behaves mainly elastically when the stress is of short-duration (e.g. seismic and tidal forces). Thus, with regards to this *short-term response* (from seconds to hours and days) to surface loads, the Earth can be approximated by a thick elastic shell (lithosphere and mantle) which surrounds the fluid core. As the load duration increases, the lithosphere continues to act as an elastic material. In contrast, the behaviour of the mantle changes from elastic to viscous and begins to behave more like a fluid than a solid. Thus, where loading occurs over extended time period (millions of years), the Earth's *long-term response* can be regarded as a thin elastic shell (i.e. the lithosphere) surrounding a viscid fluid, representing the sub-lithospheric mantle and core.

The viscoelastic response of the Earth to surface loading is a function of the Earth's rheology and the magnitude and spatial distribution of the loads. If h_i is the thickness of the ice load then the displacement u_r due to loading the Earth's surface can be approximated by a *local isostasy* model (e.g. Lambeck, 2005a)

$$u_r = \frac{\rho_i}{\rho_m} h_i \tag{4.4}$$

where ρ_i and ρ_m represent the densities of the ice and mantle, respectively. In this model, the load is supported by the buoyancy force at the base of the mantle. However, this model is unrealistic as it assumes that the lithosphere has no shear strength. Nevertheless, local isostasy can be used to estimate the magnitude of crustal deflection beneath large scale ($\gg H$, where H is the thickness of the lithosphere) and long lived ($\gg \eta/\mu$, where η and μ are the viscosity and rigidity of the mantle; the viscoelastic relaxation time, see below) ice loads. In general however, the model of *regional isostasy* is more appropriate as it assumes that the load is supported by both the elastic strength of the lithosphere and by the buoyancy forces at the base of the lithosphere (Lambeck, 2005a). The regional isostasy model provides a reasonable description of the Earth's response to surface loading on time scales longer than the relaxation time of the mantle ($10^4 - 10^5$ year).

The short- and long-term response of the Earth to surface loading represent two 'end-member' states. On intermediate time scales of around 10^3 to 10^5 years, the

initial elastic response of the lithosphere and mantle to a change in surface load is followed by a viscous flow which partially relieves the elastic stress. Hence, for intermediate load durations the viscosity of the mantle has to be taken into account since the stresses transmitted into the mantle will not have relaxed. This is particularly significant for large scale loads which induce stress deep into the mantle. With time the load-induced stresses in the viscous mantle relax and the load is increasingly supported by the combination of elastic stresses in the lithosphere and the buoyancy force within and at the base of this layer (regional isostasy model).

When the mechanical response of the lithosphere is represented by the simple model of an elastic plate overlaying an inviscid layer, the bending of the plate in response to an applied surface load is dependent on the flexural rigidity D

$$D = \frac{E\, h^3}{12\,(1-\nu^2)} \tag{4.5}$$

where h is the thickness of the layer, E the Young's modulus, and ν the Poisson's ratio. The flexural rigidity is a characteristic of the strength of the lithosphere or a measure of its resistance to bending (Walcott, 1970; Turcotte and Schubert, 2002, Chapter 3).

The flexural wavelength λ of the regional rebound of the plate in response to the load can be estimated as

$$\lambda = 2\pi \left(\frac{4\, D}{\Delta\rho\, g}\right)^{\frac{1}{4}} \tag{4.6}$$

where $\Delta\rho$ is the density contrast of the materials below and above the elastic lithosphere and g is the acceleration of gravity. The flexural wavelength of the lithosphere characterises the physical response of the layer to loading (e.g. Turcotte and Schubert, 2002, Chapter 3), the response to loading decreasing with the wavelength of the load. That is, the lithosphere filters out short wavelengths.

As mentioned in Section 4.1, the mantle has traditionally been interpreted as a linear viscoelastic body, specifically a Maxwell body in glacio-isostatic studies. This allows an additive separation of elastic and viscous strains. As stated above, in this simple description of the Earth's behaviour, the response to surface loading is characterised by an initial elastic deformation followed by stress relaxation such that the load-induced stresses in the viscous part of the body ultimately vanish. This viscoelastic behaviour of the mantle is limited by the relaxation time or so-called *Maxwell time* τ (e.g. Walcott, 1980). The Maxwell time τ is defined

as the time taken for stress to decay to $1/e$ (36.8%) of its initial value. For a model with a single viscosity η and rigidity μ, the relaxation time is η/μ. For example, for a typical upper mantle viscosity of 10^{21} Pa-s and rigidity of 10^{11} Pa the relaxation time is about 300 years. For more realistic Earth models, there is usually a spectrum of relaxation times as a function of the wavelength of the deformation (e.g. McConnell, 1968; Wieczerkowski et al., 1999).

The theoretical development of models estimating the deformation of the Earth resulting from surface loading has been attempted by a number of different investigators (e.g. Haskell, 1935; Farrell, 1972; Peltier, 1974; Cathles, 1975; Farrell and Clark, 1976). In the standard approach, the constitutive equation of the viscoelastic material is transformed into the Laplace (frequency) domain. In the frequency domain, the constitutive equation of the viscoelastic fluid is equivalent to that of an elastic material, therefore the elastic solution can be applied. The time dependence of the viscoelastic response to surface loading can be calculated when inverting from the frequency domain back to the time domain (Johnston, 1993b).

In regards to the main focus of this thesis, i.e. the Earth's and sea-level response to mountain deglaciation, the changes in ice volume of those glaciers are of small dimensions and the load duration is relatively short. Hence, although a viscoelastic Earth is used in this thesis, it is acknowledged that the response of the Earth due to changes in the load is dominated by the elastic component.

4.2.1 Earth models

Seismic observations reveal that the Earth's elastic properties vary with depth. To first order, we can consider the Earth as a layered body with smooth variations of elastic properties within the layers and abrupt changes at layer boundaries. This allows us to model the Earth as a stratified sphere whose rheological parameters are a function of depth. Although there are lateral differences in the physical properties of the Earth, a spherically symmetric model approximates the real Earth adequately for most applications if the parameters reflect the mantle state beneath the area of loading.

The determination of Earth parameters is based on interpretations of large-scale geophysical observations. These observations (i.e. sea-level histories and observations of free-air gravity anomalies) are primarily related to processes of glacial isostatic adjustment, principally associated with the advance and retreat

of Late-Pleistocene continental ice sheets. In particular, the sea-level signature at tectonically stable shorelines can be used to estimate the rheological properties of the mantle and the mechanical properties of the lithosphere (e.g. Lambeck, 1990, 1993; Lambeck and Johnston, 1998). Note that such estimates of the rheological properties assume that the spatial and temporal variations of the ice loads are understood. Another geophysical observation, the free-air gravity anomalies are expected to be negative where postglacial rebound is still ongoing, as glacial isostatic adjustment is not complete (e.g. James, 1992). Additionally, two observations of the properties of the Earth's rotational state can also be used to constrain properties of the mantle (Nakiboglu and Lambeck, 1980). These observations are the so-called nontidal component of the acceleration of the Earth's rate of axial rotation and the true secular drift of the pole of rotation with respect to the surface geography (Wahr, 1988). Seismic tomography can also be used to construct global models of mantle properties (e.g Tanimoto and Lay, 2000, and references therein).

For analyses in this thesis, the Earth is generally divided into three layers, the lithosphere and the upper and lower mantle. However, some of the Earth models used in this study also incorporate an additional layer, the asthenosphere.

The *lithosphere* is the solid outermost shell of the Earth, i.e. the crust and the uppermost mantle. The definition of the lithosphere is vague; it can be seen as a mechanical-, seismic-, thermal-, or chemical boundary layer (depending on the problem to be addressed). Here, the lithosphere is defined as a layer with a distinctly elastic mechanical behaviour compared to the predominantly viscous behaviour of the underlying upper mantle when stressed on time scales of order 10^3 to 10^5 years. This lithosphere is rarely greater than 100 km thick beneath the continents but in areas of crustal extension or hotspot activity may be only a few tens of km thick.

The *mantle* can be divided into an upper and a lower domain separated by the seismic velocity discontinuity occurring at an average depth of 670 km. Throughout the mantle lateral heterogeneities are detected with seismological observations; these are associated with deep convective processes. The upper mantle is defined as the layer between the bottom of the lithosphere and the discontinuity at 670 km. Studies on glacial rebound (e.g. Nakada and Lambeck, 1987; Mitrovica, 1996; Lambeck and Johnston, 1998) and observations of perturbations in the gravity field which are sensitive to vertical variations of viscosity in the mantle (e.g. Richards

and Hager, 1984; Hager, 1984) suggest that the upper mantle has a lower viscosity than the lower mantle (by a factor between 10 and 100).

Seismic evidence from surface waves suggests that the lithosphere is overlying a distinct seismic zone - called the *asthenosphere* - characterised by low shear-wave velocities and high seismic attenuation. As part of the mantle, this layer marks the boundary where the mantle is effectively decoupled from the lithosphere.

Only radial dependence of rheological parameters is considered in this work. The elasticity and density of the Earth are predominantly determined from modelling the propagation of seismic waves through the planet's interior. The elastic parameters and the densities for the mantle used here are based on the Preliminary Reference Earth Model (PREM) model of Dziewonski and Anderson (1981). The objective of developing the PREM model was to 'set up a standard model for the structure of the Earth, from the centre to the surface, defining the main parameters and principle discontinuities in such a way that they could be adopted by the international scientific community in any studies that depend on the Earth's structure' (Dziewonski and Anderson, 1981, p. 298). This average Earth model is a mathematical abstraction, as the lateral heterogeneity in the first few tens of kilometres is so large that an average model does not reflect the actual Earth structure at any point. However, the PREM model provides parameters as a function of radius, such as density, velocities, elastic constants, seismic quality factor Q, pressure, and gravity, that are used by a variety of geophysical, geochemical and astronomical studies.

The parameters of mantle viscosities adopted in this thesis have been found to give an adequate description of the Earth's response to ice sheet loading (e.g. Lambeck, 1990; Lambeck et al., 1998). Seven Earth models with different parameters for lithospheric thickness and upper and lower mantle viscosities are listed in Table 4.1 and will be referred to as to *ma2A*, *mb2A*, *mc2A*, *ma4A*, *ma1A*, *ma25*, and *ma2C*. Model *ma2A* is the standard model and will be used as a reference model for further comparisons. The other models represent the range of plausible values for the effective thickness of the lithosphere and the effective viscosities of the upper and lower mantle.

Additionally, four more Earth models are used in calculations within this thesis (Table 4.2). While one of these is also characterised by three layers, the other three models have a further layer, a low viscosity asthenosphere, and different parameters for the remaining three layers. The parameters of these Earth models have been endorsed by Bölling et al. (2001), Larsen et al. (2004), Larsen et al.

(2005), and Hagedoorn and Wolf (2003) on the basis of regional studies and are mainly used in Chapter 7.

	ma2A	***mb2A***	***mc2A***	***ma4A***	***ma1A***	***ma25***	***ma2C***
lithospheric thickness [km]	65	50	80	65	65	65	65
upper mantle viscosity [Pa-s] lith. - 670km	2×10^{20}	2×10^{20}	2×10^{20}	4×10^{20}	10^{20}	2×10^{20}	2×10^{20}
lower mantle viscosity [Pa-s] 670km - CMB	10^{22}	10^{22}	10^{22}	10^{22}	10^{22}	5×10^{21}	3×10^{22}

Table 4.1: Parameters for the lithospheric thickness and the upper and lower mantle viscosities of seven different Earth models used in this thesis, labelled *ma2A*, *mb2A*, *mc2A*, *ma4A*, *ma1A*, and *ma2C*.

	ma43	***mbax4A***	***maau4A***	***mdbw47***
lithospheric thickness [km]	65	50	65	110
asthenospheric thickness [km]	n/a	110	110	100
asthenospheric viscosity [Pa-s]	n/a	1.4×10^{19}	3.7×10^{18}	10^{19}
upper mantle viscosity [Pa-s] lith./asth. - 670km	4×10^{20}	4×10^{20}	4×10^{20}	4×10^{20}
lower mantle viscosity [Pa-s] 670km - CMB	3×10^{21}	10^{22}	10^{22}	7×10^{21}

Table 4.2: Parameters of Earth models used by Bölling et al. (2001), Larsen et al. (2004), Larsen et al. (2005), and Hagedoorn and Wolf (2003) labelled as *ma43*, *mbax4A*, *maau4A*, and *mdbw47*, respectively.

4.3 Sea-level response to glacial unloading

The *geoid* is the equipotential surface of the Earth's gravitational field which best fits the sea surface (ignoring oceanographic and meteorologic factors). Over land the geoid corresponds to the level water would reach in a canal that is connected to the ocean. Consequently, this equipotential surface (the geoid) that corresponds to sea level can be calculated and represented over land. For the remainder of the thesis, where sea level is evaluated over land it should be understood to be a representative of the geoid and where sea-level changes are presented over land it is the change in the geoid taking into account the deformational, gravitational, and ocean-volume change.

The shape of the sea surface is determined by the mass distribution within and on the Earth as well as by the self-gravitation of the oceans (Farrell and Clark, 1976). A redistribution of mass consequently results in variations in the shape of the sea surface, i.e. variations in the shape of the geoid (e.g. Lambeck, 1988; Conrad and Hager, 1997), and non-uniform changes of sea level along coastlines.

In the previous section, the deformation of the Earth's solid surface in response to a change in surface load assuming a Maxwell rheology was outlined. If we allow the Earth to deform under changing surface loads, the calculations of sea-level change are further complicated by the Earth's response to the change in distribution of the surface load (i.e. as the continental ice is removed and the water is added to the ocean basin; Bloom, 1967). The relative sea-level change $\Delta\zeta$ resulting from glacial unloading can be described as a combination of the following main factors:

- the addition of melt water $\Delta\zeta_e$,
- the displacement of the Earth's surface u_r,
- the changes in the geoid δN,
- the changes in the Earth's rotation $\Delta\zeta_\Omega$, and
- the tectonic contribution $\Delta\zeta_T$.

The underlying theory of the temporal and spatial variations in sea level used here has been well developed by various research groups (e.g. Cathles, 1975; Peltier, 1976; Clark et al., 1978; Peltier et al., 1978; Nakada and Lambeck, 1987; Mitrovica and Peltier, 1991; Johnston, 1993b; Conrad and Hager, 1997; Peltier, 1998; Milne et al., 1999; Mitrovica et al., 2001; Mitrovica and Milne, 2003; Lambeck et al., 2003; Kendall et al., 2005). Only a brief discussion on the different contributions is given below and for more detailed information the reader is referred to the sources listed above.

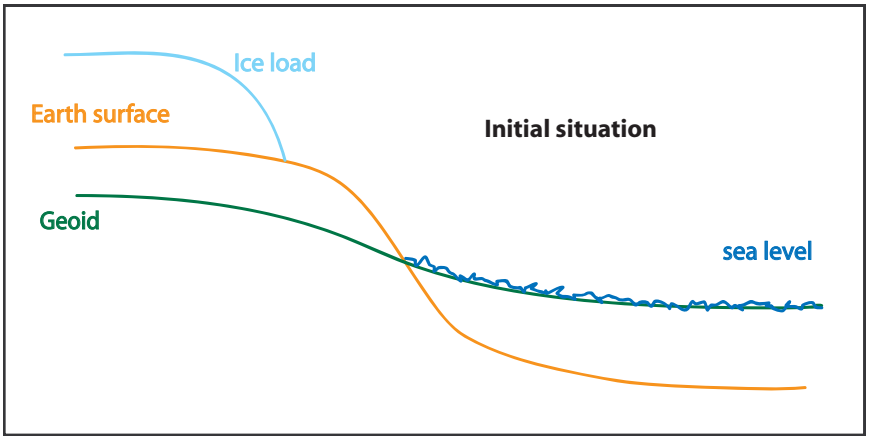

Figure 4.1: Initial ice-ocean configuration where the ice load is located close to the ocean. Mean sea level follows the geoid.

Figure 4.1 shows schematically the initial situation prior to the change in the surface load, i.e. before the ice begins to melt. Of the five factors listed above, the last one is a non-glacio-hydro-isostatic process and is not discussed here. The first four contributing factors will be reviewed in more detail below leading to the introduction of the *sea-level equation*.

1. **The distribution of the melt-water into the ocean**
   The growth or decay of land-based and grounded ice causes the ocean volume to change. In the absence of Earth deformation and changes in the gravity field, this would result in a eustatic sea-level change $\Delta\zeta_e$ which is defined as

$$\Delta\zeta_e = -\frac{\Delta V_i}{A_w} \cdot \frac{\rho_i}{\rho_w} \tag{4.7}$$

   where ΔV_i is the change in ice-volume, A_w is the area of the ocean surface and ρ_i and ρ_w are the average densities of ice and water. However, the ocean area changes as a function of time, hence a more precise definition of sea-level change is required:

$$\Delta\zeta_e(t) = -\frac{\rho_i}{\rho_w} \int_0^t \frac{1}{A_w(t')} \frac{dV_i}{dt'} dt' \tag{4.8}$$

   where A_w is the area of the ocean at time t', not including shelves covered by grounded ice. This term (4.8) represents the uniform rise in sea level that would result if the meltwater was uniformly distributed over the oceans (Figure 4.2). However, such a surface would not be an equipotential and is therefore unrealistic for representing the sea surface.

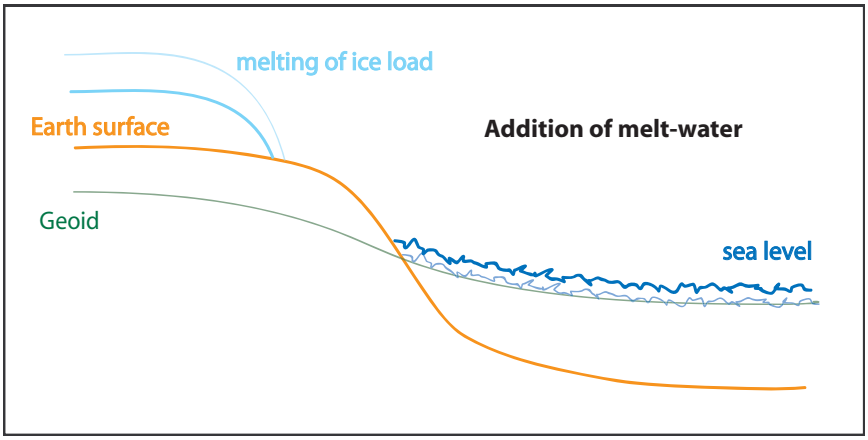

Figure 4.2: Schematic diagram of relative sea-level changes due to the addition of melt-water into the ocean. Faint and bold lines represent the ice-ocean configuration before and after the removal of land based ice, respectively.

2. **The deformation of the solid Earth under the changing surface load of ice and water**

   The response of the Earth's surface to changes in surface loads was discussed in Section 4.2. In the case of mountain glaciers of relatively small dimensions and short load durations, the stresses due to loading or unloading the Earth's surface are mostly restricted to the lithosphere, which is assumed to have a very high viscosity so that it effectively responds to the changing load as an elastic layer, although this may not be true where the lithosphere is abnormally thin.

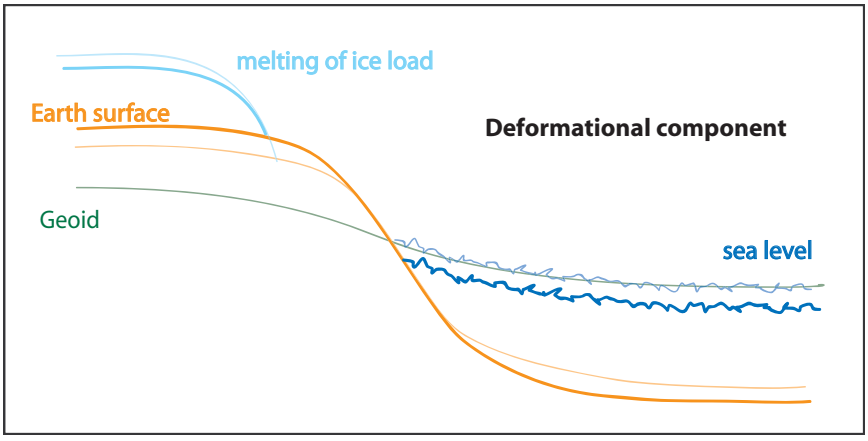

Figure 4.3: Schematic diagram of relative sea-level changes due to the deformation of the solid Earth under the changing surface load of ice and water. Faint and bold lines represent the ice-ocean configuration before and after the removal of land based ice, respectively.

The deformation of the Earth's surface results in a change in sea level (see Figure 4.3). In particular, a loss in glacier mass on land results in land uplift

beneath the load and hence in the immediate vicinity a relative sea-level fall. Furthermore, the lithosphere is loaded by the transfer of melt-water from the glacial region to the ocean. In the case of small mountain glaciers this latter factor results in only a small deformation of the ocean floor, since the amount of melt-water added into the ocean is relatively small. However, when dealing with large ice sheets, it can become quite important as discussed in Johnston (1993b).

3. **The change in gravitational potential of the earth-ice-ocean system**
   The Earth's gravity field reflects the mass distribution within the solid Earth as well as within it's oceans and ice cover. Redistribution of these surface masses (like the transfer of melt-water into the ocean) results in a change in the gravity field and hence the geoid. For the determination of the corresponding sea-level changes one can distinguish between two components:

   (a) **change in gravitational attraction due to the transfer of mass between the ice load and the ocean**
   On a rigid Earth, sea level will change due to the change in gravitational attraction of the ice-water load. At coastal sites large ice-covers attract the ocean. As the glacier melts, the gravitational attraction decreases in the near field and results in a relative sea-level fall in the vicinity of the retreating glacier (see Figure 4.4). Therefore, in regions more distant from the glaciated region, relative sea level rises. This term is a function of the temporal and spatial history of the ice load and of the geometry of the oceans.

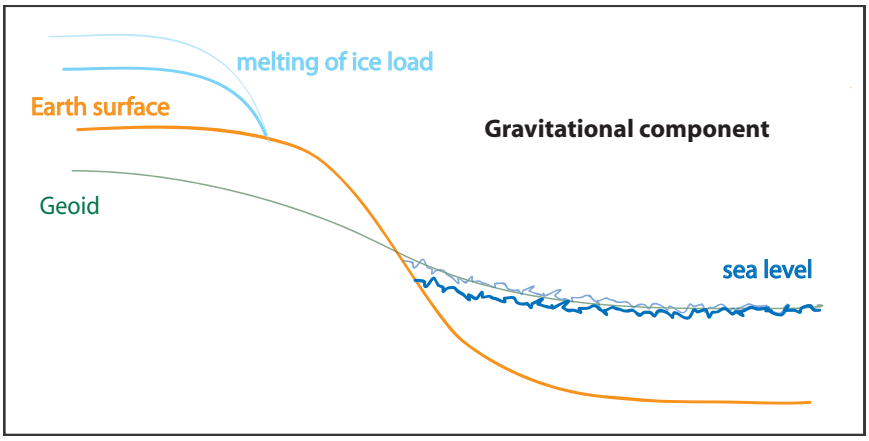

Figure 4.4: Schematic diagram of relative sea-level changes due to the change in gravitational attraction due to the transfer of mass between the ice load and the ocean. Faint and bold lines represent the ice-ocean configuration before and after the removal of land based ice, respectively.

(b) **change in gravitational attraction due to the deformation of the solid Earth**
In addition to relative sea-level changes that result from the deformation of the solid Earth (point 2. above), variations in sea-level occur as a result of the associated changes in the equipotential surfaces through mass redistribution on the Earth. In addition to the ice load fluctuations, the concomitant changes in the ocean mass distribution also stress the Earth and contribute to both radial displacements and changes in the shape of the equipotential surfaces. Hence, both the changing ice- and water load contribute to a change in the geoid (Lambeck, 1990). In the case of mountain glaciers, the changes in ice loads are relatively small and hence the deformation of the geoid (and the corresponding sea-level change) is also small.

The changes in gravitational potential of both components (a and b) result in a change in the geoid height δN. The geoid N at each point P is given by

$$N = \frac{R^2}{M_e} \left[\int_{v_e} \frac{\rho_e}{l_e} \, dv_e + \int_{v_i} \frac{\rho_i}{l_i} \, dv_i + \int_{v_w} \frac{\rho_w}{l_w} \, dv_w \right] \tag{4.9}$$

where R is the mean radius of the Earth, M_e is the mass of the Earth and the three integrals are over the volume of the solid Earth (v_e), ice sheet (v_i), and the oceans (v_w), and ρ_e, ρ_i, and ρ_w are the corresponding densities. In the first integral, l_e is the distance from the point P at which N is defined to the solid Earth, in the second integral l_i is the distance to the ice mass and in the third integral l_w is the distance to the water. The first integral represents the change in gravitational attraction due to the deformation of the solid Earth. Whereas the second integral represents the change in gravitational attraction due to the removal of ice-mass on land, the third integral incorporates the change in gravitational potential resulting from the addition of water into the oceans.

4. **The change in the Earth rotation**
Sea-level changes in response to variations in the Earth's rotation can be observed at high frequencies, such as the 14 month pole tide or Chandler-tide (Lambeck, 1980, Chapter 6.2). Such change can also occur due to the past and present-day redistribution of mass within and on the surface of the Earth (Mitrovica and Milne, 2003). In particular, the rate of rotation and the orientation of the rotation axis with respect to the solid Earth

change with time (e.g. Lambeck, 1980; Wahr, 1988; Mitrovica et al., 2005; Martinec and Hagedoorn, 2005). Astronomical observations indicate a slow drift of the rotation axis, at a rate of about $0.003''$ year^{-1} and along the longitude of $\sim$70°W. This true polar wander is usually attributed to the on-going adjustment of the planet's mantle to the last deglaciation. Astronomical observations also indicate that the Earth is undergoing a slow secular deceleration, part of which can be attributed to a response to the last deglaciation. However, this rate of about 5×10^{-22} radians s^{-2} (Lambeck, 1977) is too small to have a significant effect on sea level and the major rotational effect is attributed to the shift in the position of the rotation axis (Lambeck, 2005b, unpublished). Changes in the equipotential surface (the geoid) resulting from rotational variations can be calculated for each point P as

$$\Delta N_\Omega = \frac{1}{g} \left[\Omega^2 l dl \; + \; \Omega l^2 d\Omega\right] \tag{4.10}$$

where dl is the change in the distance l of the point P to the rotation axis and $d\Omega$ is the change in the rate of rotation Ω about the axis. Since mean sea level corresponds to the geoid, the above defined changes in the equipotential surface ΔN_Ω correspond to sea-level changes $\Delta\zeta_\Omega$. These changes in the equipotential surface are a function of mass variations within and on the Earth and are therefore dependent on the Earth rheology and the loading history of the ice masses.

Lambeck (1980) provided a first assessment of the impact of land ice melting on both the nontidal acceleration and polar wander with focus upon small ice sheets and glaciers. He estimated a change in the rotation of $0.0004''$year^{-1} in a direction 45° East (Lambeck, 1980, p. 274). Peltier (1988) calculated the perturbations of Earth rotation caused by the annual loss of 31 glaciers around the world but also included the contribution that result from the melting of the Greenland and Antarctic ice sheets.

The sea-level equation

Having defined all contributing factors, the *sea-level equation* can be formulated as

$$\Delta\zeta = \Delta\zeta_e + u_r + \delta N + \Delta\zeta_\Omega \tag{4.11}$$

where $\Delta\zeta_e$ represents sea-level changes due to the addition of meltwater, u_r is the change in sea level due to the deformation of the Earth's surface, and δN and $\Delta\zeta_\Omega$ represent sea-level changes due to changes in the geoid and the Earth's rotation, respectively.

The two terms u_r and δN can be re-grouped according to their primary sources (Lambeck et al., 2003) which are *(1)* caused by the change in ice load - the *glacio-isostatic component* -

$$\Delta\zeta_i = (u_r + \delta N)_i \tag{4.12}$$

and *(2)* caused by the change in ocean load - the *hydro-isostatic component* -

$$\Delta\zeta_w = (u_r + \delta N)_w \tag{4.13}$$

The terms $(u_r)_i$ and $(u_r)_w$ describe the deformation of the crust under the weight of the ice and water, respectively, while the terms $(\delta N)_i$ and $(\delta N)_w$ describe the change in the shape of equipotential surfaces due to the redistribution of the ice and water loads, respectively. Thus, the *sea-level equation* can also be formulated as

$$\Delta\zeta = \Delta\zeta_e + \Delta\zeta_i + \Delta\zeta_w + \Delta\zeta_\Omega \tag{4.14}$$

All these components vary spatially and temporally in different ways, and this deceptively simple equation hides a number of other complications. For example, both isostatic terms are functions of the rheological properties of the Earth and their quantifications require a realistic description of the density, elastic, and viscosity distribution within the lithosphere and mantle. The glacio-isostatic term $\Delta\zeta_i$ is also a function of the temporal and spatial distribution of the ice loads. This term plays a larger role at locations near or within the margins of former ice loads. Hence, a high-resolution description of the changes in ice loads through time is required to estimate this contribution (Lambeck, 1990). The evaluation of the hydro-isostatic term $\Delta\zeta_w$ requires a description of the ocean basin which is a function of time as the underlying sea floor deforms and as the ocean surface expands or contracts through a glacial cycle. $\Delta\zeta_w$ is a function of the planet's response to the ice load, hence $\Delta\zeta_w$ is a function of the sea-level change itself. For example, near the ice loads where the water level is pulled up by the gravitational attraction of the ice, the local rise is greater than at sites far from the ice, where the eustatic sea-level term $\Delta\zeta_e$ gives a closer approximation of the actual change. The evaluation of $\Delta\zeta_w$ therefore requires a knowledge of sea-level change and the solution of Equation 4.14 requires multiple iterations. Finally, while the ice-volume-

equivalent sea-level term ($\Delta\zeta_e$), as defined by Equation 4.8, appears to be a function of time only, the time dependence of the shorelines and of the ice grounding lines means that this term also has a weak dependence on both the Earth's rheology and on the loading history of the ice masses (Lambeck, 2005b, unpublished).

In conclusion, estimating relative sea-level changes due to changes in surface loads requires that all terms of the sea-level equation (Equation 4.11 or 4.14) are considered. Since the deformational component of the sea-level equation is caused by the displacements of the Earth's surface, these land movements Δz (measured positive upward) are given by

$$\Delta z = -u_r \tag{4.15}$$

and can be monitored using geodetic techniques (e.g. Milne et al., 2001). The spatial and temporal variability of the deformation of the Earth's surface is therefore dominated by the deformational component as shown in Figure 4.3.

Numerical modelling of the sea-level response to glacial unloading - the *calsea* program

In order to solve the sea-level equation, a *spherical harmonic* approach has been used at the ANU to develop the sea-level program *calsea* (Johnston, 1993a,b; Lambeck et al., 2003). This program was primarily developed to constrain both the rheology of the Earth and the melting history of past ice sheets from the theory for the deformation of a self-gravitating, compressible and viscoelastic sphere under a surface load. In this thesis, this forward modelling technique is used to calculate relative sea-level changes due to recent mountain deglaciation. Regional isostatic response (see page 112) followed by viscoelastic relaxation is implemented in the *calsea* program through the Earth models used in this thesis (see Section 4.2.1). Since mathematical modelling of the behaviour of a spherical body is most conveniently undertaken in spherical polar coordinates, spherical harmonic functions after Johnston (1993a) are used. The higher the spherical harmonic expansion, the greater the spatial resolution with which the load is defined. This is particularly important for mountain glaciers of small areal extent. The maximum degree of expansion used here is 256 corresponding to a wavelength of approximately 150 km. Because of the attenuation effect of the lithosphere of short wavelength components in the load solutions, higher degree expansions are not required (unless the lithospheric thickness is less than $\sim$50 km). As a linear viscoelastic response model is adopted in the *calsea* program, there is a

linear dependence of the solution to the magnitude of the loading over its history (Lambeck and Johnston, 1998). A constant change in height of the load over the entire history will scale the response by the same factor. Changing only part of the load history will produce a more comprehensive change of the response because of the viscoelastic "memory".

The ocean function in the *calsea* program is based on the coefficients of the surface spherical harmonic expansion of Munk and MacDonald (1960). Non-uniform water loads resulting from the distribution of melt water are accounted for (Johnston, 1993b). Furthermore, as sea level changes, the position of the shorelines moves and this is also considered in the program (Lambeck et al., 2003). To solve the sea-level equation, several iteration steps are needed since, as mentioned earlier, the hydro-isostatic component is a function of the sea-level curve itself. In conclusion, to calculate the sea-level response to glacial unloading, Earth-, ice-, and ocean models are required as well as the Earth's response function.

4.3.1 Sea-level changes due to mountain deglaciation: a case study of Svalbard

In the previous section, the sea-level equation was developed and its various contributions were discussed. In this section, global mountain deglaciation based on $T_G P_{Z\&O}$ (Section 3.1.1) is applied and the various contributions are presented in a case study of Svalbard (a more detailed description on the method used to implement the ice-volume changes into the *calsea* program is given in Chapter 5). In addition to the various individual contributions, the impact on estimates of relative sea-level changes using different Earth models is discussed.

4.3.1.1 Contributors to relative sea-level changes

The actual locations of glaciers where ice-volume changes are taking place are unimportant when considering the contribution to global ocean-volume change since it is assumed that all glacier-melt ultimately goes into the oceans. However, when studying local sea level or crustal rebound on a regional scale, the locations of the changing glaciers become important. For all calculations in this section the standard Earth model *ma2A* (Table 4.1) is used.

Figure 4.5 shows a cross-section of cumulative modelled relative sea-level changes over the period 1871-1990 along 79°N (over land, represented by the brown line,

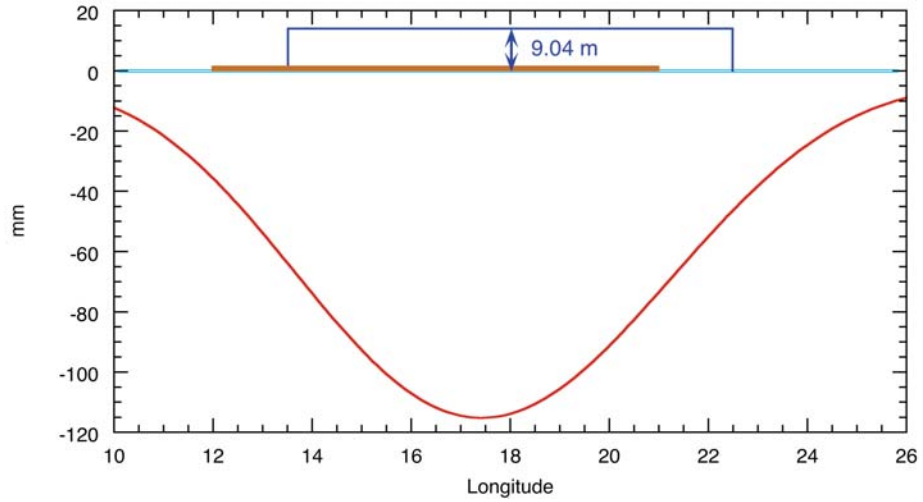

Figure 4.5: Modelled relative sea-level changes along 79°N in mm over the period 1871-1990 due to global recent mountain deglaciation. The glacier in Svalbard covers an area of 36,600 km^2 approximated by a square and loses 9.04 m (water equivalent) in height over the entire period. The brown line indicates the land along 79°N.

these relative sea-level changes correspond to changes in the geoid, see Section 4.3). Globally, glaciers contributed 7733 km^3 of water to the ocean over the 120-year period and over 330 km^3 of this melt-water came from glaciers of the Svalbard archipelago with an area of 36,600 km^2. However, a significant local fall in sea level of up to 115.2 mm is computed within the margins of the glacier over the period 1871-1990. The slightly asymmetric signal of relative sea-level change in Figure 4.5 (the modelled form of the changing glacier is symmetric about 18°E) is caused by the different land-ocean distribution to the East and West, i.e. the coast lines at 79°N run approximately through 12 and 21°E.

Figure 4.5 illustrates that the ability to measure this signal at geodetic sites is dependent on the distance of the observational site from the glacier and the total change in ice-volume. As described in Section 4.3, the spatial variation of relative sea-level changes consists mainly of the following components:

1. **Addition of melt water** $\Delta\zeta_e$
   The first component of added melt-water to the ocean obtained for a global data set of mountain glaciers is 7733.46 km^3 of water, which is equivalent to 21.36 mm of eustatic sea-level rise over the period 1871-1990. With an estimated ice-volume loss of 330.91 km^3 w.e. (equivalent to a global sea-level rise of 0.91 mm) from the glacier in Svalbard, the added melt-water from that single glaciated region represents over 4% of the total estimate from global mountain deglaciation.

2. **Deformational component** u_r

   The spatial variation in relative sea-level changes due to the deformation of the solid Earth in Svalbard is shown in Figure 4.6. In this case, changes in relative sea level of -97.4 mm over the period 1871-1990 are predicted in the centre of the glacier. This indicates that the deformational component accounts for about 85% of the predicted total signal of sea-level fall at that site.

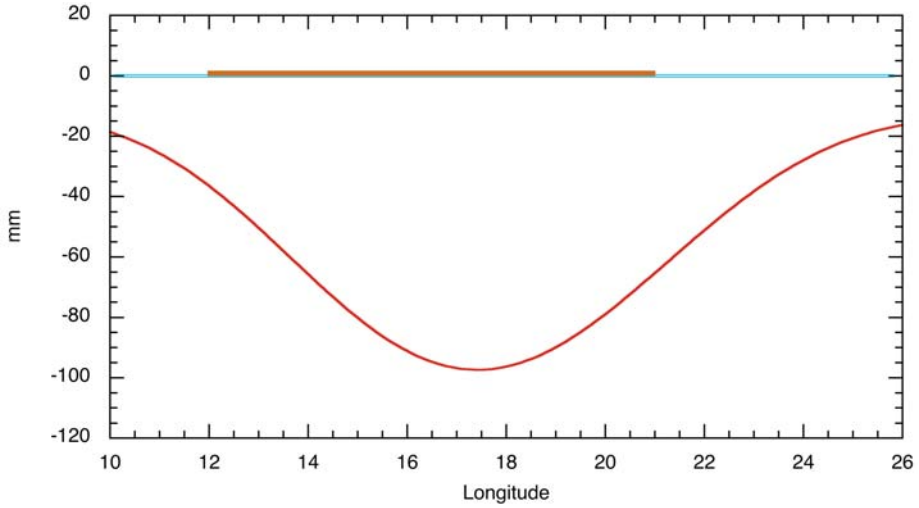

Figure 4.6: Modelled relative sea-level changes in Svalbard along 79°N in mm over the period 1871-1990 due to the deformation of the solid Earth caused by recent mountain deglaciation. The brown line indicates the land along 79°N.

3. **Gravitational component** δN

   The third component of relative sea-level changes is caused by the change in gravitational potential, shown in Figure 4.7 for the case study of Svalbard. Figure 4.7a shows relative sea-level changes resulting from the change in gravitational attraction of the ice-water load. The maximum change in relative sea level in Svalbard is -20.1 mm over the period 1871-1990 (equals $\sim$17% of the total signal at that site). Figure 4.7b shows relative sea-level changes due to the change in gravitational potential caused by the deformation of the solid Earth. The change in relative sea level here is minor as the size of the ice load is relatively small. For Svalbard, the maximum change in relative sea level that is caused by the change in gravitational potential due to the deformation of the solid Earth is estimated to be 2.0 mm over the period 1871-1990.

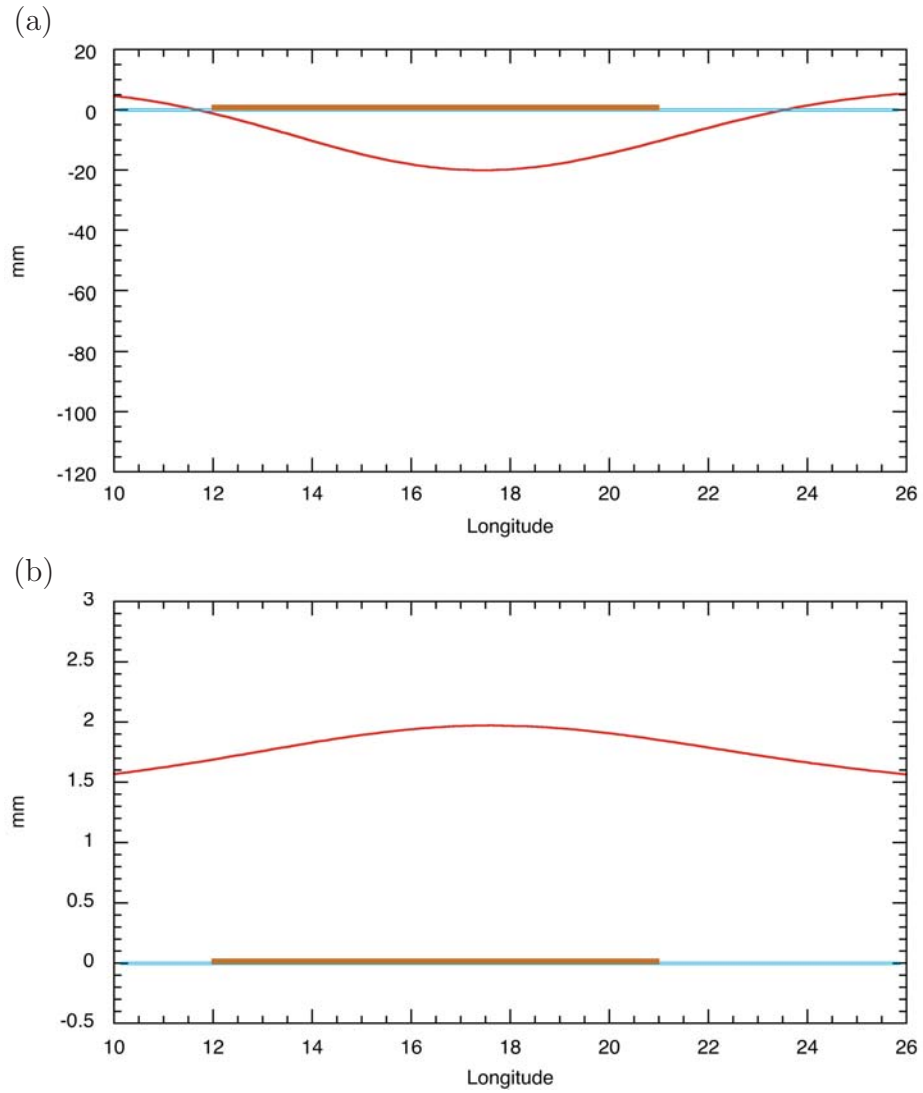

Figure 4.7: Modelled relative sea-level changes in Svalbard along 79°N in mm over the period 1871-1990 due to (a) the change in gravitational attraction of the ice-water load and (b) the change in the gravitational potential due to the deformation of the solid Earth as a result of recent mountain deglaciation. The brown line indicates the land along 79°N.

4. **Rotational component $\Delta\zeta_\Omega$**
   Considering the rotational component when calculating relative sea-level changes due to recent mountain deglaciation results in variations in the estimates. In particular, comparison of modelled relative sea-level changes at existing tide gauge stations with and without considering the rotational component show a maximum difference of ± 0.01 mm year^{-1} at sites in mid-latitudes. Nevertheless, this small number indicates that the rotational contribution to relative sea-level changes in consequence of recent mountain deglaciation is negligible.

The sum of all above components (1. to 4.) results in the estimate of the relative sea-level changes in Svalbard shown in Figure 4.5. The individual calculations listed above demonstrate that the pronounced spatial variation in Figure 4.5 is predominately due to a combination of the deformation of the solid Earth and the change in gravitational attraction between the glacier and the ocean.

Vertical land movements can be immediately obtained from these results. As noted in Equation 4.15, vertical land movements are equal to the opposite sign of the deformational component. This is illustrated in Figure 4.8 where the predicted maximum vertical land uplift in Svalbard is found to be 97.4 mm.

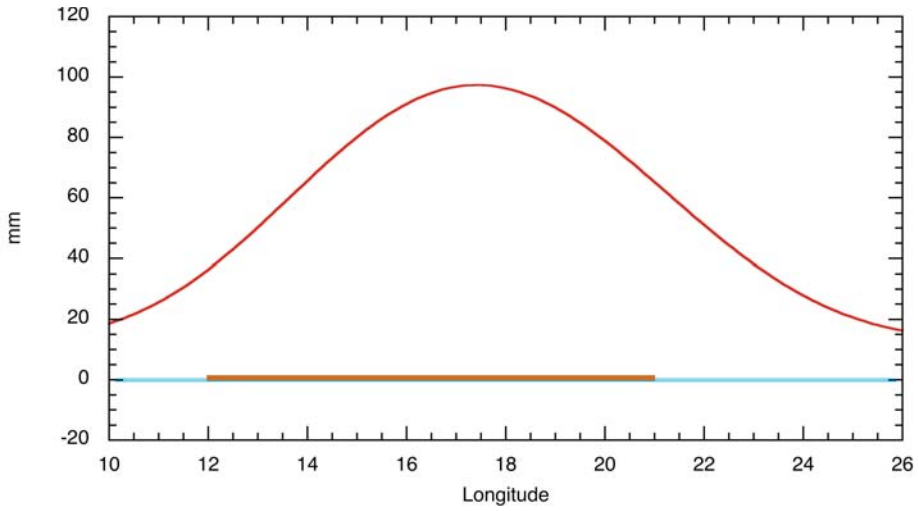

Figure 4.8: Modelled vertical land uplift in Svalbard along 79°N in mm over the period 1871-1990 as a result of recent mountain deglaciation. The brown line indicates the land along 79°N.

When dividing the sea-level equation into its sources (Equation 4.14), the glacio-istostatic and hydro-isostatic components are calculated and are shown in Figure 4.9 for the case study of Svalbard. The curves illustrate that in the near field the glacio-istostatic contribution $\Delta\zeta_i$ has a greater effect than the hydro-istostatic

term $\Delta\zeta_w$. The asymmetric signal in the hydro-isostatic component is caused by different spatial distributions of water loads, e.g. land at latitude 79°N lies mostly between 12 and 21°E.

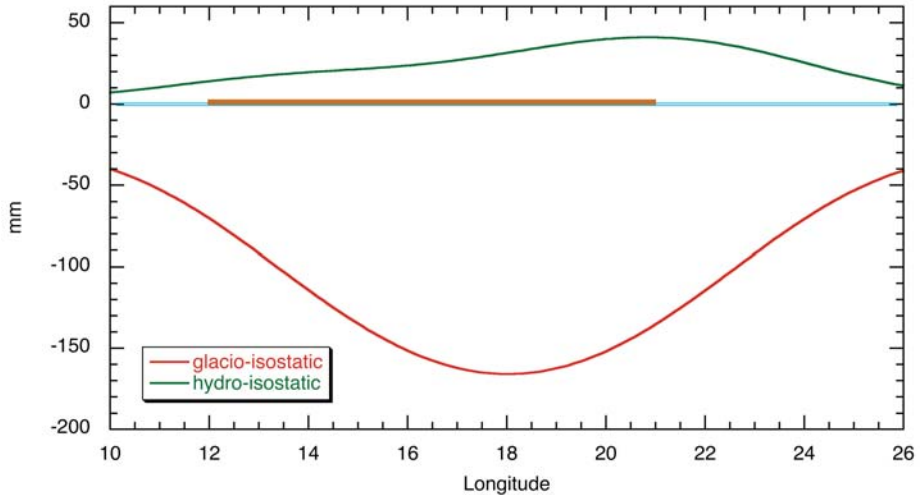

Figure 4.9: Glacio-isostatic and hydro-isostatic components of sea-level changes in Svalbard along 79°N in mm over the period 1871-1990 due to recent mountain deglaciation. The brown line indicates the land along 79°N.

Combining the glacio- and hydro-isostatic components of Figure 4.9, and the contributions to the eustatic sea-level with the rotational components, results again in the total predicted sea-level curve of Figure 4.5.

4.3.1.2 Dependence on Earth models

In all calculations discussed in the previous sections, the standard Earth model *ma2A* was applied to represent the Earth rheology world wide. However, the Earth's structure in different regions, e.g. Alaska and Svalbard, may vary. To assess the degree of variation in relative sea-level changes using various Earth models, ten further models have been used to calculate geodetic signal. Detailed parameter descriptions on all Earth models are listed in Tables 4.1 and 4.2 (Section 4.2.1). Compared to the standard Earth model *ma2A*, the models *ma1A* and *ma4A* have different viscosities in their upper mantle and the models *mb2A* and *mc2A* have different lithospheric thicknesses. Models *ma2C* and *ma25* are characterised by different lower mantle viscosities. Model *ma43* has different parameters for both upper and lower mantle viscosities than the standard model. Three further models incorporate an additional layer (low viscosity asthenosphere).

Figure 4.10 shows estimates of relative sea-level changes due to recent mountain deglaciation at two tide gauge sites in Alaska (Yakutat and Cordova) and one site in Svalbard (Ny Ålesund) using different Earth models in the calculation. The dashed horizontal lines represent the results using the standard Earth model *ma2A*. Models to the left to the vertical blue line in Figure 4.10 have three layers, defined by a lithospheric thickness and an upper and a lower mantle viscosity (Table 4.1 and 4.2). The variations in relative sea-level using these Earth models show that changing the viscosity of the lower mantle and changing the thickness of the lithosphere result in no significant variation in the magnitude of sea-level changes, compared to the standard model. This independence of these results is caused by the relatively small size of ice loads compared to the thickness of the lithosphere and the short loading history. The biggest change in relative sea level produced by using different three-layer Earth models results from varying the upper mantle viscosity, in particular using a lower value for its viscosity (*ma1A*). However, this stronger signal in the magnitude of relative sea-level changes is not as pronounced at the Ny Ålesund site. Overall, using different three-layer Earth models to calculate relative sea-level changes produces only minor variations in estimates. At permanent tide gauge stations located close to the glaciated regions in Alaska and Svalbard, plausible deviations from model *ma2A* result in differences in the geodetic signal of no more than 7%. Differences of the same order are expected at other geodetic sites around the world.

Results to the right of the vertical blue line in Figure 4.10 use Earth models that include a low viscosity asthenosphere (Table 4.2). Here, the predicted sea-level changes at the three sites are all greater than when using the standard model. In particular, an increase in the signal of up to 80% is derived at the Yakutat tide gauge station. This illustrates that the introduction of a low viscosity asthenosphere in the Earth model can result in more pronounced variations of geodetic signals and also that the difference is more dependent on the location of the site than it is in the case of three-layer models.

In these models, the low viscosity zone is intended to be local, restricted to the region under investigation (such as the plate boundary region of Alaska). In contrast, the rheological model used in the *calsea* program is global and does not handle local changes. Implications of the low viscosity zone on geodetic results may be accurate in the local region under consideration but not in the far field (where the hydro-isostatic component will be incorrect). In the case of mountain glaciers, the loads are of small horizontal dimensions and small amplitude. Since

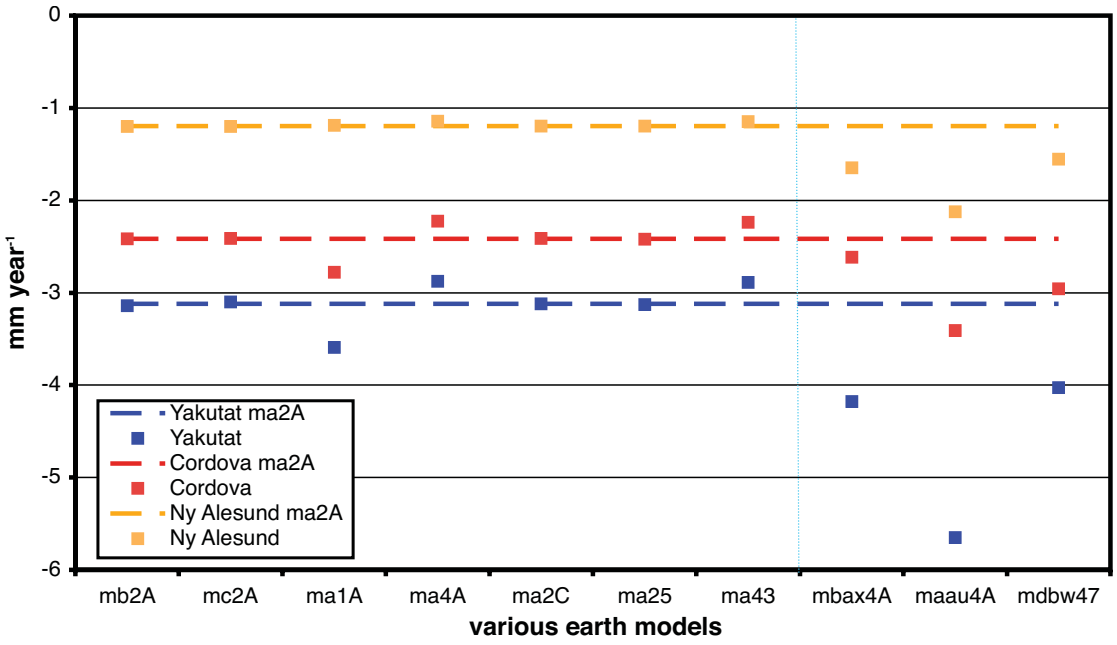

Figure 4.10: Estimates of relative sea-level changes in mm year^{-1} over the period 1961-1990 due to recent mountain deglaciation at tide gauge stations in Alaska (Yakutat and Cordova) and Svalbard (Ny Ålesund) using various Earth models. The dashed, horizontal line at each site represents the predicted sea-level change when using the standard Earth model *ma2A*.

the majority of the deformational and gravitational changes are localised, the model results are valid within the local region (Lambeck, 2005b, unpublished). Hence, using global models to represent the local response to small loads within the region of the low viscosity zone is valid.

4.4 Summary and conclusions

Sea-level changes resulting from melting of mountain glaciers are not globally uniform. This is mainly due to two factors: the deformation of the crust under changing surface loads and the change in gravitational attraction due to the change in the ice-water load. Both processes can be significant in the neighbourhood of the melting glaciers. Additionally, a change in the equipotential surface results from the deformation of the solid Earth. This change in the geoid also produces sea-level changes. The simple estimated eustatic sea-level change (as a result of the added meltwater of glaciers) is therefore not an adequate estimate of regional sea-level changes.

Part of the regional sea-level signal results from vertical land movements. Therefore, this signal is a relative measurement and observations made at tide gauge sites can only be used to derive accurate global changes when corrections are applied.

This chapter has demonstrated that relative sea-level changes and vertical land movements near large glacier systems are of magnitudes that could possibly be observed with geodetic techniques, such as tide gauge, GPS, and VLBI (Very Long Baseline Interferometry) measurements (e.g. Altamimi et al., 2002; Holgate and Woodworth, 2004). Conversely, this opens the possibility of using these observations to constrain the glacier history.

Analyses using different Earth models showed that the projected sea-level response is not only dependent on the amount of ice melted, but also on the Earth rheology that is assumed. In turn, it may be possible to constrain regional variations in rheology from the Earth's response to mountain deglaciation. Due to the relatively short loading histories, the effective viscosity constrained by recent mountain deglaciation is probably higher than those determined by from glacial isostatic rebound of past deglaciation histories. However, this conclusion is only possible if the loading history and the local tectonic activity are accurately constrained.

The predicted global and regional patterns of geodetic signals (relative sea-level changes and vertical surface deformation) due to recent mountain deglaciation will be described in detail in the following chapter.